# Evolution of the mechanisms of asymmetric spindle   positioning in nematode embryos

Tanmaya Sethi

BS-MS 5th year

20131132

Supervisors: Dr. Chaitanya Athale (IISER, Pune, India)

Dr. Marie Delattre (ENS, Lyon, France)

# Certificate

This is to certify that this dissertation entitled "Evolution of the mechanisms of asymmetric spindle   positioning in nematode embryos" towards the partial fulfillment of the BS-MS dual degree programme at the Indian Institute of Science Education and Research, Pune represents study/work carried out by "Tanmaya Sethi (Registration No. 20131132) at Indian Institute of Science Education and Research, Pune and École normale supérieure de Lyon, France" under the supervision of "Dr. Chaitanya Athale, Associate professor, Division of  Biology, IISER, Pune and Dr. Marie Delattre, LBMC, ENS de Lyon" during the academic year 2017-2018.
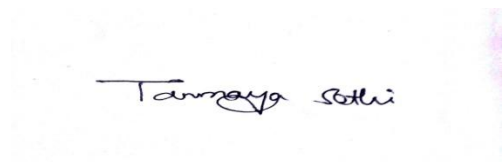
Student: Tanmaya Sethi
Regd.No: 20131132

Supervisor
Dr. Chaitanya Athale
Associate Prof,
IISER,Pune

Supervisor
Dr. Marie Delattre
Team Leader
LBMC, ENS, Lyon

# Declaration

I hereby declare that the matter embodied in the report entitled "Evolution of the mechanisms of asymmetric spindle positioning in nematode embryos" are the results of the work carried out by me at the Department of Biology, IISER Pune and LBMC, ENS de Lyon under the supervision of Dr. Chaitanya Athale and Dr. Marie Delattre and the same has not been submitted elsewhere for any other degree.

Student : Tanmaya Sethi
Regd. No: 20131132

Supervisor
Dr. Chaitanya Athale
Associate Prof,
IISER,Pune
20/03/2018

Supervisor
Dr. Marie Delattre
Team Leader
LBMC, ENS, Lyon
21/03/2018

# Abstract

Asymmetric cell division is essential for generating cellular diversity, which leads to two unequal daughter cells with different cellular fates. In most of the animal cells, asymmetric spindle positioning is the key factor which leads to the first asymmetric cell division and decides the size of the daughter cells. Although the process of asymmetric positioning of spindle is conserved in most of the species, but not much is known about the robustness of the mechanisms which lead to this evolutionarily conserved phenomenon. We recorded the first embryonic division three nematode species such as *Caenorhabditis elegans*, *Oscheius tipulae and Diploscapter sp.*JU359 to study the biophysical properties of spindle positioning and the mechanical parameters those can affect the spindle positioning. We hypothesized that viscosity could be one of the parameters which might affect the different mechanisms which govern the asymmetric spindle positioning. So, by using microrheology methods we tried calculating viscosity values of the cytoplasm of these nematode species by tracking the lipid granules in the cytoplasm. The results showed us that, *Diploscapter sp.*JU359 which has the least movement of spindle has the highest viscosity values and all the three species show higher viscosity values than water.

## List of Figures

# Acknowledgments

# Contents

## 1. INTRODUCTION:

The cleavage plane during animal cell division is determined by the position of mitotic spindle and thus it determines the size of the two daughter cells (Glotzer, M. (2001). So, the spindle positioning during the end of mitosis is essential for the fate of the daughter cells and whether the division will be symmetric or asymmetric. Asymmetric cell division is required for tissue homeostasis and development and relies on the asymmetric positioning of the mitotic spindle in animal cells. The one-cell embryo of the nematode (*Caenorhabditis elegans*) has been instrumental to study this process since it undergoes the first cell division which is asymmetric in size. Interestingly, many of the nematode species also undergo a first asymmetric embryonic division. By combining computational modelling, cell biology and evolutionary biology, we will attempt to explore the mechanisms of asymmetric spindle positioning in evolutionary related species of nematodes, based on a purely mechanical model and what are the mechanical parameters that influence asymmetric cell division.

*Caenorhabditis* belongs to a large group of bacteriophagous nematodes called rhabditis, which spans a huge amount of genetically and ecologically diverse species. During early development of these species, polarity establishment, asymmetric division and acquisition of cell fates are the critical steps. In case of first asymmetric cell division in the *C.elegans* embryo, the local inactivation of acto-myosin cortical contractility breaks the cell symmetry. It also helps in the establishment of PAR proteins` and other associated components` polarized distribution on the cell cortex along the longitudinal axis of the embryo, which later becomes the anterior-posterior (A-P) axis. After that, the A-P polarity is maintained through the anterior and posterior cortical domains` reciprocal negative interactions. The mechanisms which are followed for the proper positioning of the mitotic spindle and the centrosomes in the one-cell embryo by exerting pulling forces on the astral microtubules are still being studied.  A ternary complex comprised

of Gα (GOA-1/GPA-16), LIN-5 and GPR-1/2 is essential for anchoring of dynein (the motor protein) to the cell cortex. It is thought that these motor proteins exert pulling forces on the depolymerizing astral microtubules at the cortex. These complexes are slightly enriched at the posterior cortex, which leads to the asymmetric displacement of the spindle during anaphase (Colombo et al, 2003). The motors are also distributed on the lateral cortex, leading to different kinds of oscillations (Pecreaux et al, 2006)

Recently, different mechanical optimizations have been reported by the lab of Dr. Marie Delattre at ENS, Lyon that have emerged over a short evolutionary time scale to achieve asymmetric spindle positioning (Farhadifar et al, 2015) Spindle motion, likely depends on a combination of forces: pulling forces acting on each centrosome that are influenced by different material properties of the central spindle itself. This has led to the hypothesis that evolutionary change in the tuning of this machinery- the respective contribution of these forces- may have led to different spindle motion over the course of nematode evolution.Thus, the essential cellular function like asymmetric cell division gets maintained over the period of evolution while the underlying mechanisms for the maintenance of the same function (e.g. asymmetric spindle positioning) do change rapidly. With this project, we propose an integrative approach- applying simulations of spindle movements in this evolutionary framework- to uncover the biophysical features that are constrained during evolution, and the ones that are prone to drift. A computational model of the asymmetric forces acting on the *C. Elegans* spindle has been developed using the software Cytosim that invokes a combination of force generators and asymmetric cortical rigidity (Kozlowski et al, 2007). Combined with simulations of centrosomal positioning in *Xenopus* extracts and mouse oocyte (Khetan et al, 2016) in the lab of Dr. Athale, it has demonstrated the role of a balance of forces required to position and transport centrosomal MT asrters. To get the posterior displacement and oscillation, which is seen in case of most of the nematode embryos, we have to take both *in silico* and *in vivo* scenario into consideration.

## 2. MATERIALS AND METHODS:

### 2.1 *in silico* modeling of the spindle:

Cytosim, a cytoskeleton simulation engine written in C++ (Developed by Nedelec Laboratory, EMBL) was used for the simulations.

This simulation engine is based on Langevin dynamics, molecular diffusions, transient binding between them and the calculation of all forces exerted on the fibers and the molecular complexes. Using this program, we will simulate parameter changes to phenocopy the different species and identify the parameters that may have evolved. We will also validate the model *in vivo* by affecting some parameters of the system in embryos, when modifiable.

### 2.2 Worm strains and maintenance

The Bristol, i.e. N2 line was used as the *C. elegans* WT reference strain. And for *O. tipulae,* CEW1 line was used. All the strains were cultured on Nematode Growth Media (NGM) plates and they were fed with OP50 (*E. coli)* at $20^0$C.

### 2.3 One cell embryo preparation for imaging

For DIC Microscopy, young adults were transferred from NGM gar plates to M9 medium in a watch glass. Each worm was dissected using a binocular magnifier in order to free the embryos. One cell embryos were selected and transferred on a 2% agarose pad on a microscope glass slide and covered with a coverslip.

### 2.4 Microscopy of beads and embryos

DIC time-lapse movies were recorded at room temperature ($23^0$C) using an Axioimager A2 Zeiss (oil immersion objective lens 100X) and KAPPA camera. Images were taken every 0.5 second and 0.01 second for recording cell division and tracking respectively. The TIFF files were then stacked on ImageJ v 1.48d.For analysis convenience, all

embryos were oriented so that the anterior pole (where the polar body is extruded) was place on the left and posterior pole on the right.

For the control experiments, stock solutions were made of different w/w concentration of glycerol (0%, 25%, 50 % and 100%) and fluorescent NIST micro beads (1um diameter) were added to the stock solutions in 1:200 proportion. The sample solutions were put on the glass slide in a closed flow chamber and covered with cover slips. Then they were observed under the microscope (Nikon .60X oil immersion objective, N.A = 1.95).

## 2.5 Image analysis

For the control experiment data set images were taken every 0.5 seconds for 1 minute and were processed using Fiji.  For tracking, manual tracking and Mosaic tool suit plug-in were used. The embryos were recorded with time interval of 0.5 seconds and 0.01seconds for looking at the cell division and tracking respectively.

## 3. RESULTS:

### 3.1 Microscopy of first asymmetric cell division in nematode embryos

The lab of Dr. Marie Delattre have looked at the first embryonic division of 42 nematode species which are closely related to *Caenorhabditis elegans*, which also serves as an excellent model system to study the biophysical properties of asymmetric spindle positioning in these species. These studies correspond to 127 strains from 27 *Caenorahbditis* and 15 non-*Caenorhabditis* species which constitue powerfull collection of different phenotypes to study the evolutionary mechanisms underlying in various cellular processes across these species. Out of all those species we decided to work with 3 different species for their unique patterning of spindle motion. The following species are as such:

*Caenorhabditis elagans:* It undergoes its first asymmetric cell division by showing transverse oscillations (also called `rocking motion`) of the spindles.

*Oscheius tipulae*: It undergoes its first asymmetric cell division by showing longitudinal oscillations of the spindles.

*Diploscapter sp.*JU359: This species undergoes its first asymmetric cell division with the least amount of movements of the spindles.

Figure 1. **Comparison of first asymmetric cell division in nematodes**.DIC images of the first asymmetric cell division in case of the three nematode species leading to two unequal sizes of daughter cells (denoted by comparatively larger anterior to posterior cell) has been shown. The scale bar denotes 10 microns length. The outer line in case of the embryos denotes the egg shell. The black arrow heads point to the centrosomes and the black lines to the spindles.

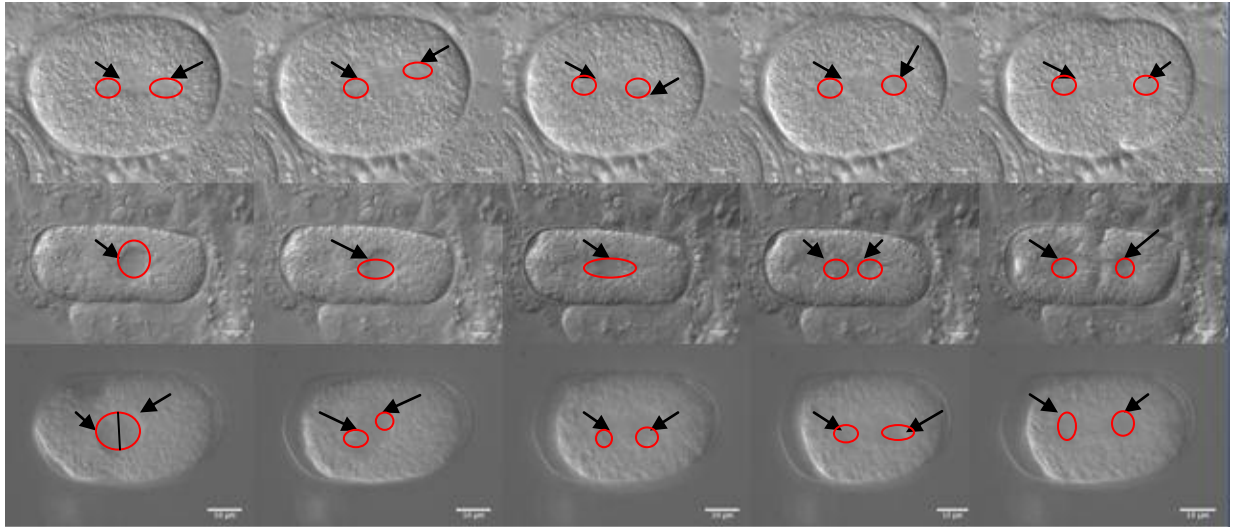## 3.2 Pattern of spindle motion in these embryos



Figure 2 **Time lapse images of the first asymmetric division demonstrating the spindle oscillation**. This figure demonstrates the sequential events till the first asymmetric division in case of the three nematode species. The red hollow ovals show the spindle poles and the black arrowheads imply their motions. A) First panel shows the rocking motion of spindles in case of *C.elegans*. B) Second panel shows the first asymmetric cell division in case of *Diploscapter* species without any significant oscillatory motion of the spindles. C) The third panel shows the longitudinal oscillations denoted by the black arrow marks in case of *Oscheius tipulae*. The scale bars are of 10microns denoted by white line below the time lapse images in each panel.

The spindle movements in case of the three species have been shown in figure 2, where it can be inferred the rocking motion of the spindles in case of *C.elegans,* the longitudinal motion in case of *Oscheius tipulae* and barely any movement of the spindle in case of *Diploscapter.* On an average 20 movies per each species were recorded for the further processing.

### 3.3 Potential mechanical parameter to describe the uniqueness

Speculating about the mechanical parameters that could lead to these different patterns of oscillations and eventually asymmetric cell division, one parameter that was taken into account was viscosity. As the movie recordings of the first cell division of the three species showed some kind of differences in Cytoplasmic viscosity (indicated by the granular density in figure 3), we decided to proceed towards measuring viscosity values of these species using microrheology.



Figure 3 **Comparison of granular density across the three species.** The figure shows the zoomed in version of the granular density in case of *C.elegans, O. tipulae* and *Diploscapter.* The scale bars are 10 microns.
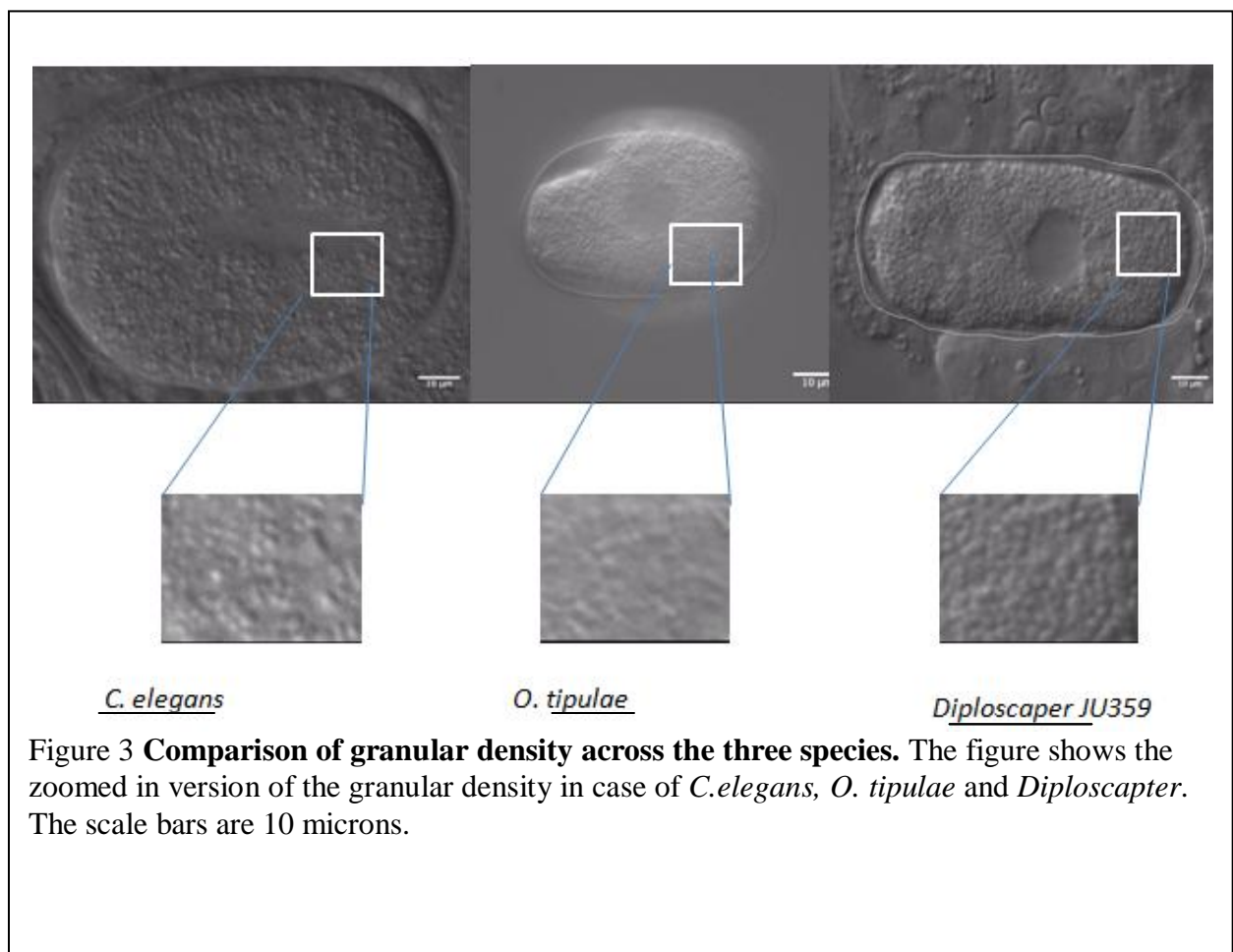
Cytoplasmic viscosity in case of these three species looks different as we can refer from figure 3 ,where it looks like *Diploscapter* has the highest granular density as compared to the other two species, which might contribute to the different pattern of spindle motion and oscillations seen in case of these three species. And, these granules undergo Brownian motion as shown in figure 4.



Figure 4 **Tracking of single particles in case of three species.** The figure shows the manual tracking of granules in case of the three nematode species. The trackings show Brownian motion.
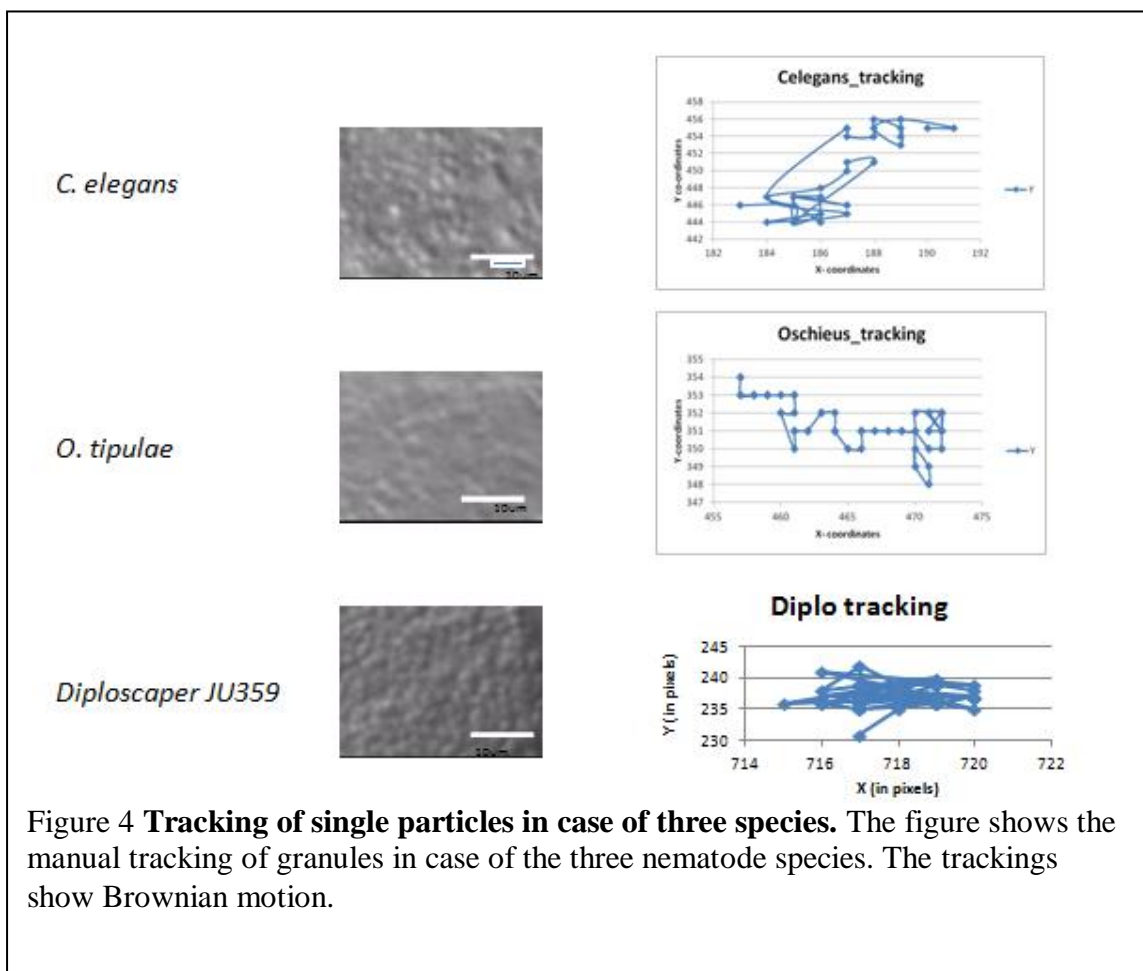
## 3.4 Measurement of parameter viscosity using microrheology

The approach that we used for the calculation of viscosity is as follows:
The particles (beads for control calculations and lipid granules for *in vivo*
experiments) were tracked both manual and automated using Mosaic tool using the
time series recordings of the samples in Fiji. Then, from the tracking results Mean
Square Displacements were calculated using different methods, from the MSD plots
diffusion coefficients (D) were calculated. And, from these diffusion coefficients,
viscosity values were calculated for different sample solutions using Stoke- Einstein
Equation which is given by the following expression.

$$D = \frac{RT}{N6\pi\eta a} \qquad (1)$$

where R is universal gas constant, T is the temperature, N is Avogadro`s number,
η= dynamic viscosity and a is the radius of the particle which is different for different
sample.

## 3.5 Calculations of viscosity using beads in solutions:

Control experiments were done using nano and micro beads in different solutions
whose viscosities are already known e.g Water, different glycerol w/w concentrations.
The sample solutions (0%, 25%, 50%, 60% glycerol w/w ) were made and the
fluorescent  micro beads( with 1micron diameter) were added to the solutions and
observed under the microscope for 1 minute with a time lag of 0.5 sec between each
frame.

0% glycerol 25% glycerol

50 % glycerol 60% % glycerol
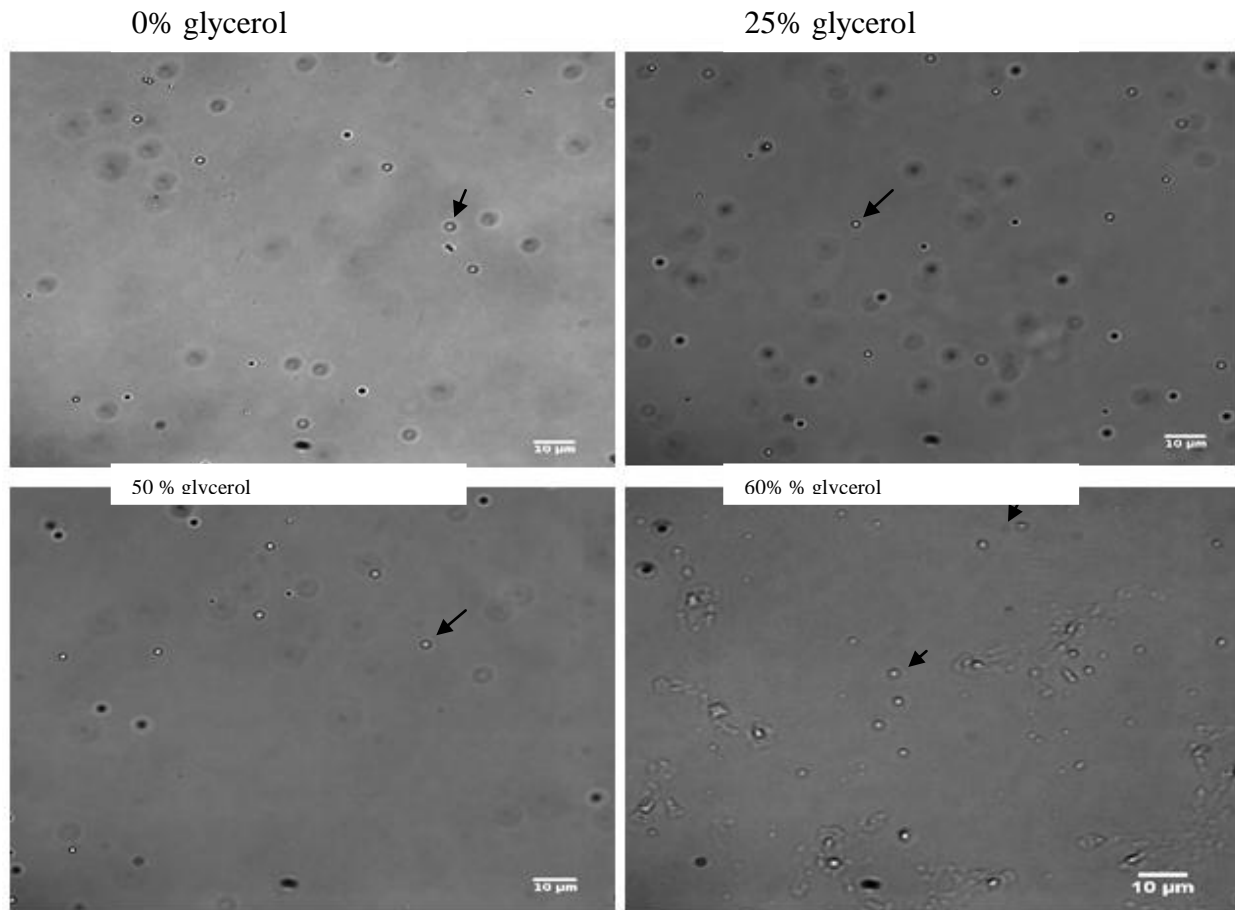
Figure 5 shows the microscopic image of the beads (denoted by black arrowheads) in different solutions.

The recordings were analyzed using Fiji and the beads were tracked manually. The results of the tracking data were saved in a matrix form of time, x-coordinate and y-coordinate for on an average 80 frames. For the calculations of MSD, the msdanalyzer (Tarantino et al, 2014) package of MATLAB, Anomalous method and Drift model (previously established by Neha Khetan at Dr. Chaitanya Athale`s lab).

According to the anomalous method, Diffusion co-efficient can be calculated from the following equation:

$$\langle r^2 \rangle = 4 \, D'.t^\alpha \qquad (2)$$

Where r is the displacement, D' is the diffusion co-efficient, t is the time step and α is the anomaly parameter.

The drift model for calculation of diffusion co-efficient is as follows:

$$\langle r^2 \rangle = 4. D_{eff}. \delta t + \left( v_{eff}. \delta t \right)^2 \qquad (3)$$

Where $D_{eff}$ is the diffusion co-efficient, δt is the time increment and $v_{eff}$ is the velocity term.
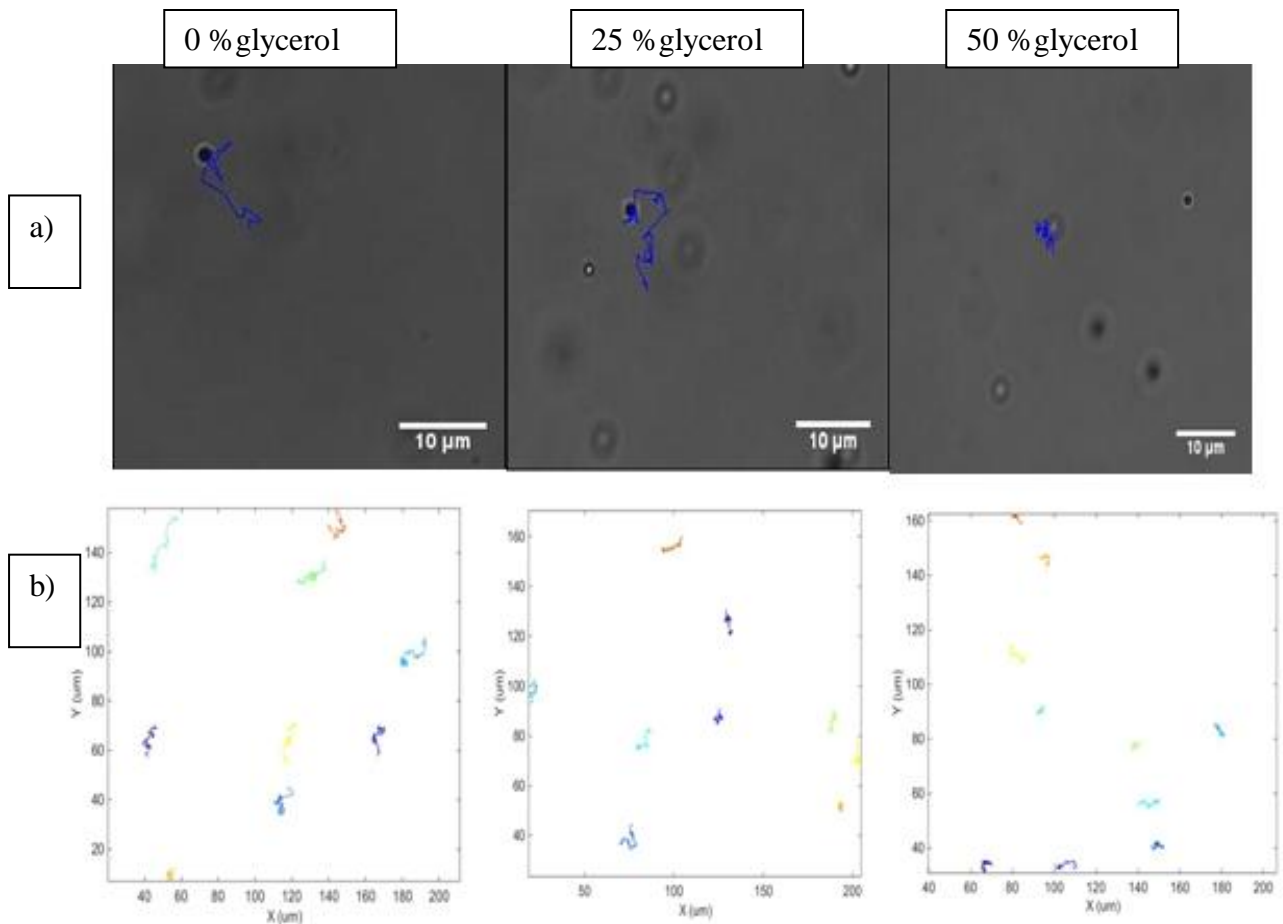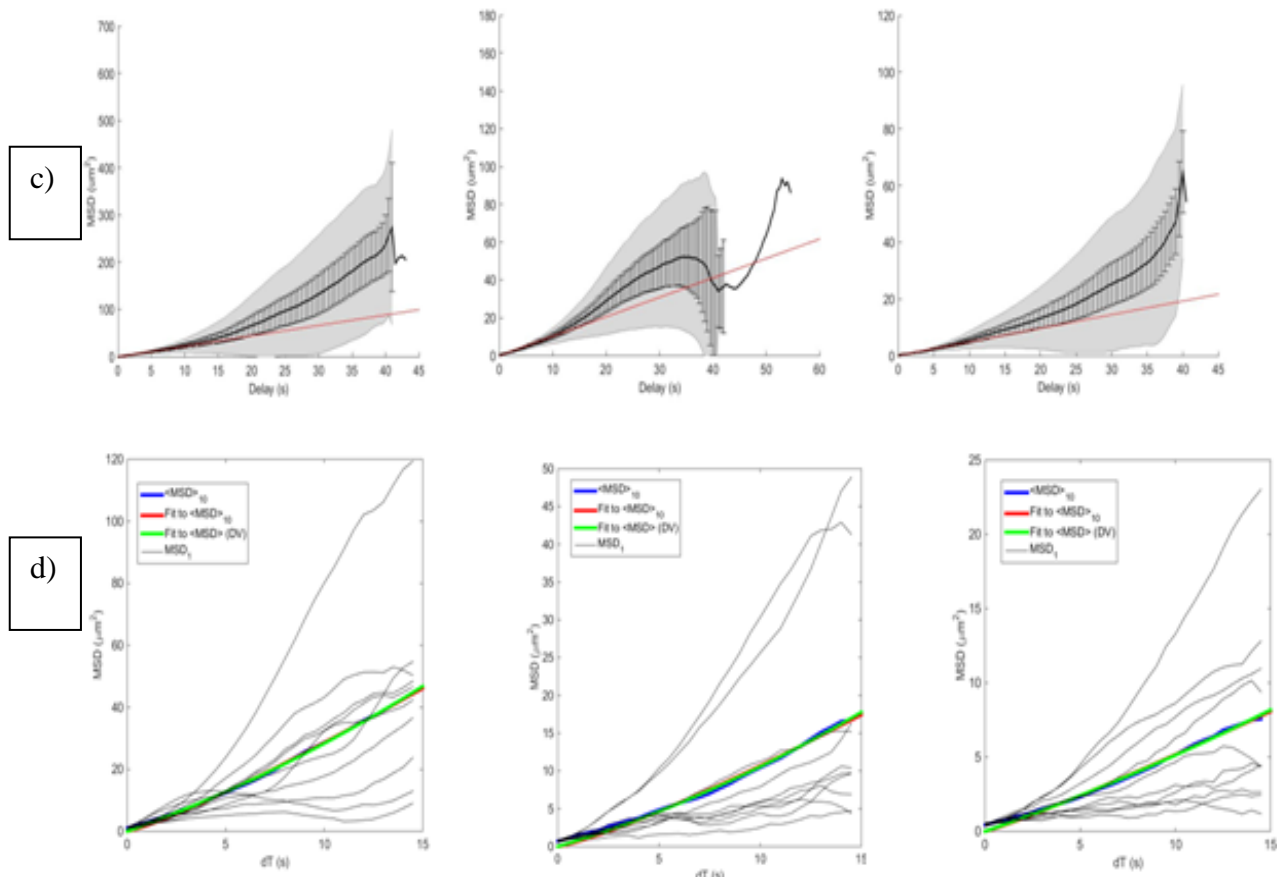
**Figure 6 MSD calculations for control experiments using three different methods.**
Panel a) shows the tracks followed by a single bead which are denoted by the blue lines in case of water, 25% glycerol and 50 %glycerol respectively. Panel b) shows the XY trajectories followed by 10 beads in case of the three sample solutions. Panel c) shows the individual MSD plots for all the 10 beads for each sample solutions. Panel d) shows the mean MSD curve and the fit of all the 10 individual MSD plots calculated by msdanalyzer (black line), by anomalous method (red line) and by drift model (green line). Scale bar = 10 microns

To calculate the diffusion co-efficient for the sample solutions, the slopes of the mean MSD plots were calculated from their fits. Then, the viscosity values were calculated using the Stoke- Einstein equation and were compared with the reported (known) viscosity values. The results are shown in the following table1.

Table 1. **Comparison of viscosity values of different concentration of glycerol solution**:

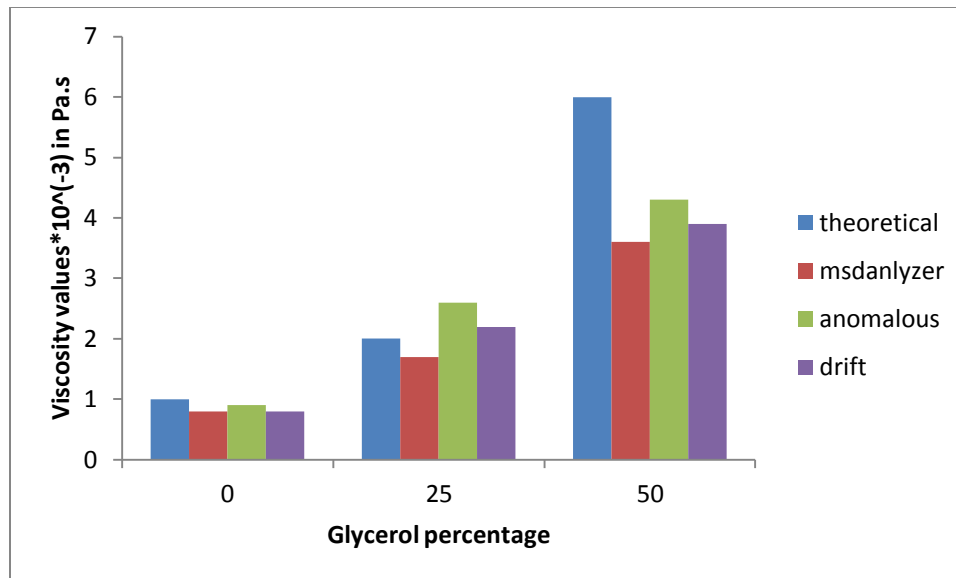| Percentage of Glycerol | Theoretical viscosity values (in Pa.s) | Viscosity value (by msdanalyzer method ) in Pa.s | Viscosity value (by anomalous method ) in Pa.s | Viscosity value (by drift method ) in Pa.s |
|---|---|---|---|---|
| 0% (water) | $1.008*10^{(-3)}$ | $0.8*10^{(-3)}$ | $0.9*10^{(-3)}$ | $0.8*10^{(-3)}$ |
| 25% | $1.75-2.5*10^{(-3)}$ | $1.7*10^{(-3)}$ | $2.6*10^{(-3)}$ | $2.2*10^{(-3)}$ |
| 50% | $6*10^{(-3)}$ | $3.6*10^{(-3)}$ | $4.3*10^{(-3)}$ | $3.9*10^{(-3)}$ |

Figure 7.**comparison of different η values calculated by three methods.**
The results from table1 are shown in the bar graphs in figure 7. The blue bars denote the theoretical (reported) values of viscosities for different glycerol concentrations. The red bars from msdanalyzer code, the green bars from anomalous method of MSD calculations and the purple bars are the viscosity values calculated from the drift model.

From the above calculations the results from all the three MSD calculation methods, the viscosity values are quite comparable with the theoretical values. So, we can use these methods as proxies to calculate the viscosity values for the three nematode species.

### 3.6 Calculations of viscosity of the cytoplasm of the nematode species

The young adults of the nematode species were taken into account for the experiments. The worms were kept on the glass slide immersed in M9 solutions and they were cut into two halves so that the embryos will come out of the gonads and will be in the solutions. The embryos were collected from the solutions using a mouth pipette and were placed on agar base on the glass slide. Then, they were covered with the coverslip to be processed under the microscope (100X oil immersion objective).The images were taken every 0.01 second for the tracking of granules. Images were processed using Fiji for the manual Tacking using the Manual tracking plug-in. The results were saved in the similar fashion of the control experiment data set for further

calculation of MSD. The following figure shows the results of the MSD calculations for the three nematode species.
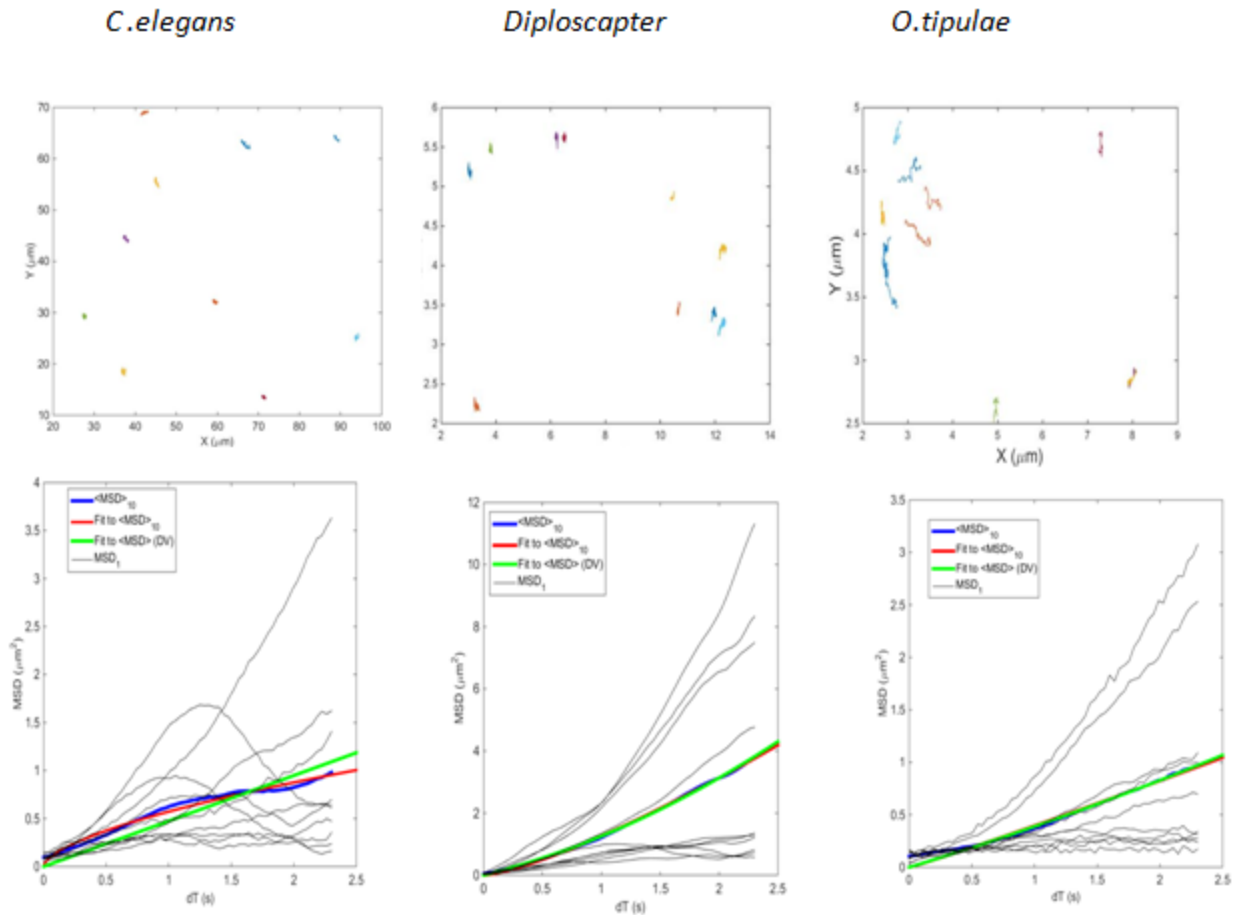


Figure 8 **MSD calculations of three nematode species**. Figure shows the XY trajectories of 10 lipid granules of the three nematode species over 80 frames, individual MSD curves for each granule, mean MSD from each species respectively. The results are shown in table 2.

Table 2 : Comparison of viscosity values from three methods

| Species name | Viscosity from msdanalyzer method(in Pa.s) | Viscosity from anomalous method(in Pa.s) | Viscosity from drift method(in Pa.s) |
|---|---|---|---|
| *C.elegans* | 2.9*10^(-3) | 2.5*10^(-3) | 3*10^(-3) |
| *O. tipulae* | 1.4*10^(-3) | 1.1*10^(-3) | 1.5*10^(-3) |
| *Diploscapter sp.JU359* | 5.7*10^(-3) | 2.9*10^(-3) | 3.2*10^(-3) |
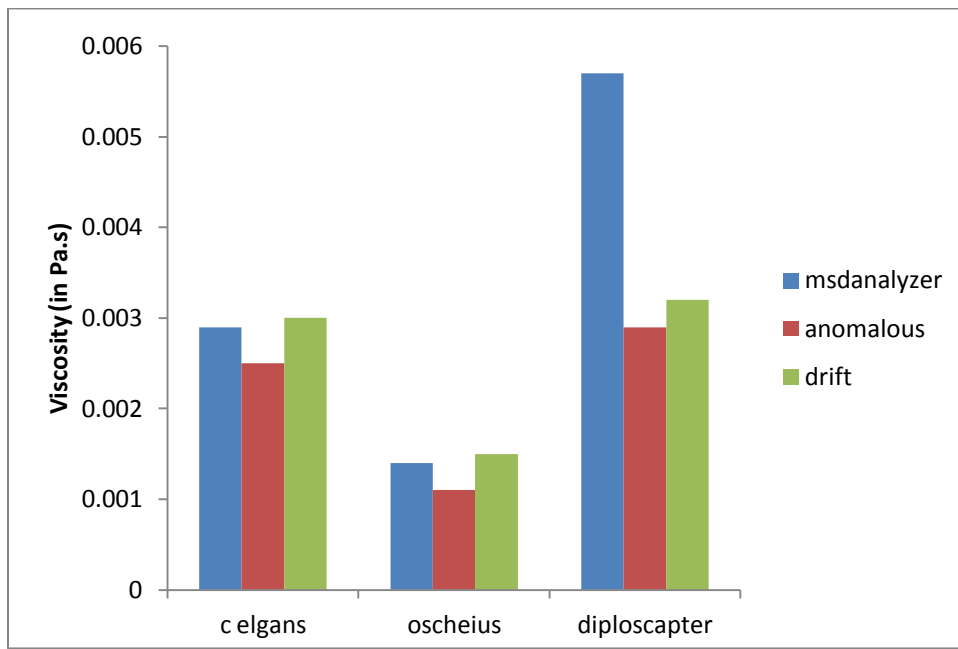


Figure 9 shows the bar graph representation of the results obtained from table 2, which shows significant difference between the values obtained by msdanalyzer and the other two methods( anomalous and drift). These results however match with our hypothesis regarding *Diploscapter* having higher viscosity values compared to the other two species.

So, to check for more potential mechanical parameter which can affect the spindle oscillations, we can check the effects of these parameters in an *in vitro* scenario to have

an idea about the combinatorial effect of the parameters. So, we tried approaching the problem in an *in silico* manner.

### *3.7 in silico approach*:

First, we tried mimicking the standard model given by Nedelec et al (2007) for *C. elegans* embryo by using the source code of Cytosim. To do that, I learned some basics of simulations and how to use the software Cytosim during the start of the project (Figure 1). Then, to approach our problem we tried playing with several parameters and added them to the code. We also identified ways to quantify the outputs of the different simulations, in order to compare them with the results which can be obtained from live imaging of nematode embryos. The results from these exercises follow this section.

### 3.8 Parameters affecting the spindle motion in simulation

The parameters which are required for the simulation (with reference to Kozlowski et al, 2007) have been listed in Table 3.

| Parameters | Values ( Kozlowski et al,2007) | Parameter corresponding in Cytosim | Reference |
|---|---|---|---|
| Asymmetry | posterior is 50% softer | | |
| Viscosity | 1 pNs/ µm*2 | | Daniels et al., 2006 |
| MT growth speed | 0.51 µm/s | Growing_speed | Srayko et al.,2005 |
| MT shrink speed | 0.84 µm/s | Shrinking_speed | |
| MT catastrophe rate | 5/s | Catastrophe_rate | |
| Fiber Rigidity | 120 pN/ µm*2 | rigidity | Dogterom and Yurkey,1997 |
| Cytoplasmic | 0.01/s | | |

| | | | |
|---|---|---|---|
| catastrophe rate | | | |
| Cortical Rigidity | 370(P) and 560(A) pN/µm*2 | | |
| Force generator attachment rate | 5/s(posterior) and 3.2/s(anterior) | | |
| Force generator detachment rate | 0.003/s | | |
| FG/ Cortex combined Elasticity | 370 pN/µm | | |
| Force generator characteristic force | 28 pN | | |

Table 3 refers to the parameter of values used in the Cytosim simulation of spindles in *C. elegans*

Simulation outputs:
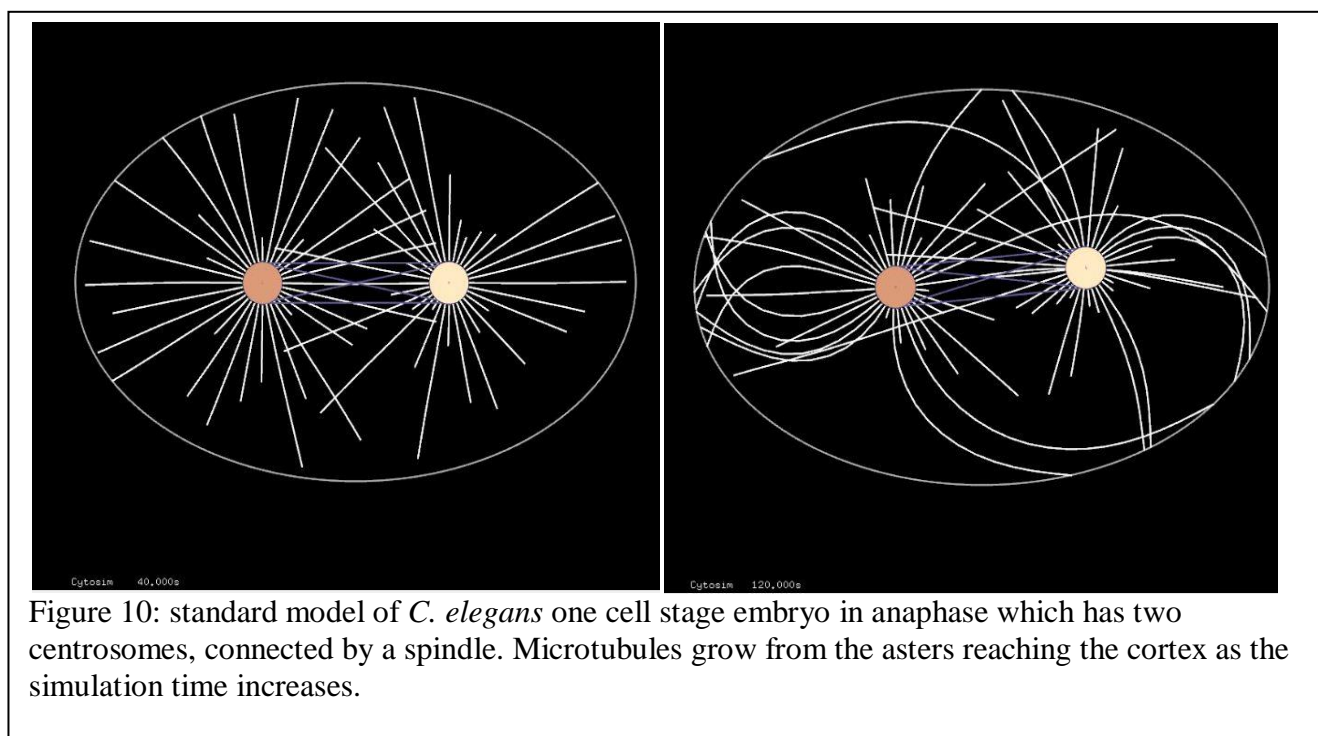### 3.9 Standard *C. elegans* model:



Figure 10: standard model of *C. elegans* one cell stage embryo in anaphase which has two centrosomes, connected by a spindle. Microtubules grow from the asters reaching the cortex as the simulation time increases.

For grafted dyneins:

## 3.10 Effect of Force generators at the cortex:

After mimicking the standard model, the next step towards the problem was to introduce force generating complexes into the system. As dyneins are the major components of the Force generator complexes, which help in exerting forces on both the poles, we tried putting dyneins at the cortex by playing with the parameters. These dyneins are called grafted dyneins as they are grafted to the cortex using parameters (like `grafted` and `edge`) in the code. This scenario was simulated in both 2D and 3D cases (Figure 11).
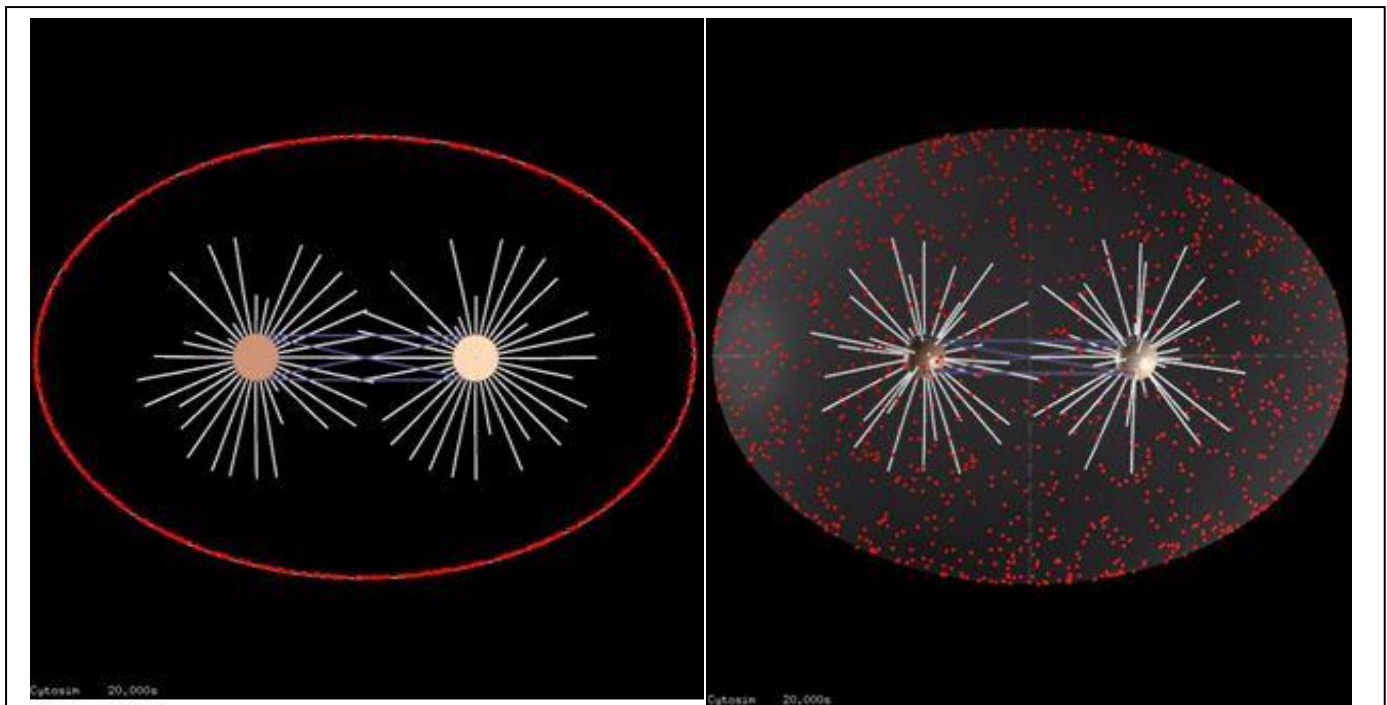


*Fig11.* Represents an embryo having two centrosomes connected by a spindle where the red dots represent the grafted dyneins in 2D and 3D respectively.
No. of frames= 40, no. of fibers = 32 and ρ (density) = 6/μm*3

### 3.11 Spindle movements:

After putting grafted dyneins at the cortex, the next aim was to look at the effect of these complexes on the movement of spindles.

Microtubules reach to the cortex as the simulation time increases (Figure 3). The spindle poles move asymmetrically i.e. one pole moves faster and more than the other one. Asymmetric oscillations can be seen in case the spindle poles without even putting any asymmetry in the code. One pole moves more vigorously and shows oscillations compared to the other one which is stochastic in every simulation, so we can`t orient the cell`s anterior and posterior axis as of now. And, that is why the spindle poles are represented as class id1 and class id2 for analysis (instead of anterior and posterior pole).

The FG/cortical rigidity (in this case represented by dynein stiffness) is a parameter which represents the combined stiffness of the force generators and the cortex, which is also inversely proportional to the oscillations speed of the pole according to Kramer`s law[3]. The value of this cortical rigidity was kept symmetric throughout the cortex in this case i.e       370    pN/µm
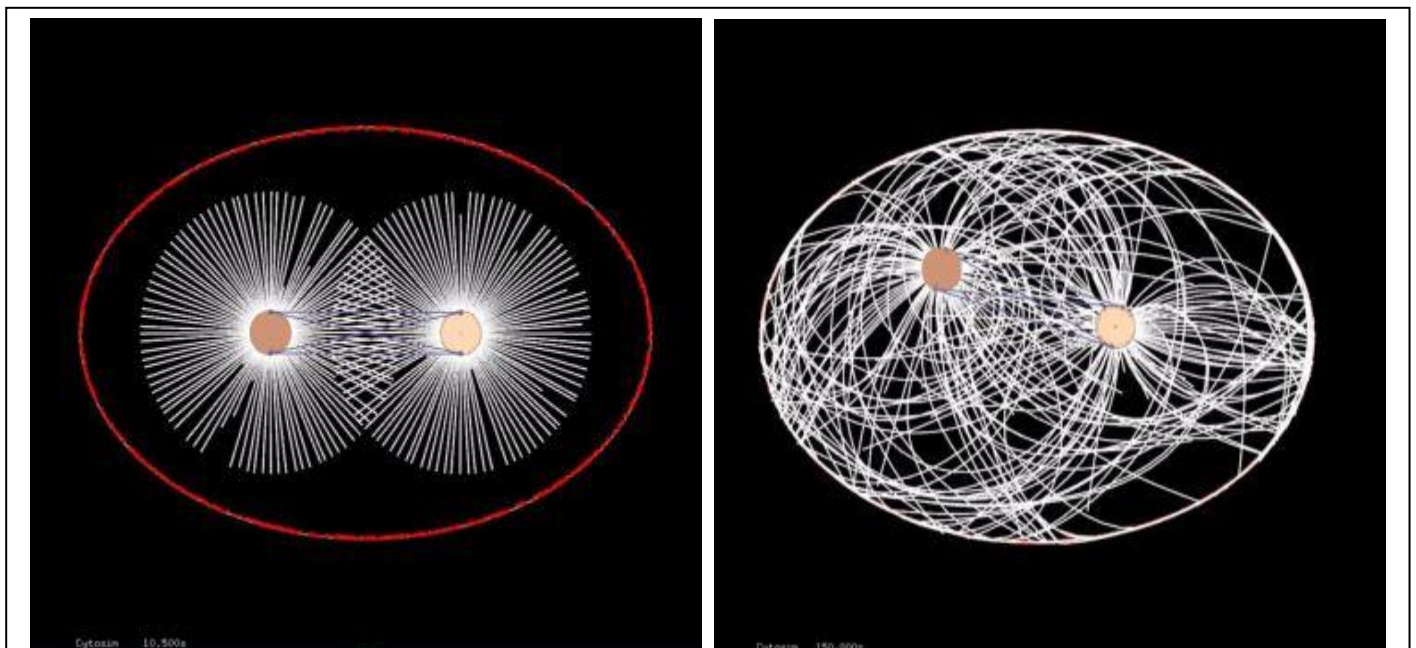


*Fig 12*: a) shows the start of the simulation and b) at the end of 150 seconds of the simulation time. Where    class    id-1=centrosome,    class    id-2=centrosome,    class    id-3=    spindle    and Dynein stiffness: 370 pN/ µm. The spindle shows some kind of oscillations which might be intrinsic to the model.

**3.12 Quantitative interpretation of the spindle oscillations:**

After getting the outputs from the simulations, to make a sense of the phenomenon, their quantification was needed. To do the quantification, we tried representing the trajectories of the cell components (such as spindle poles, spindles) in both Cartesian co-ordinates (Figure 4) and Polar co-ordinates (Figure 5), which will help us further in the quantitative analysis.

The trajectories of both the poles were traced in XY co-ordinates through the simulation time. One of the two poles was seen moving vigorously as compared to the other and having oscillations.
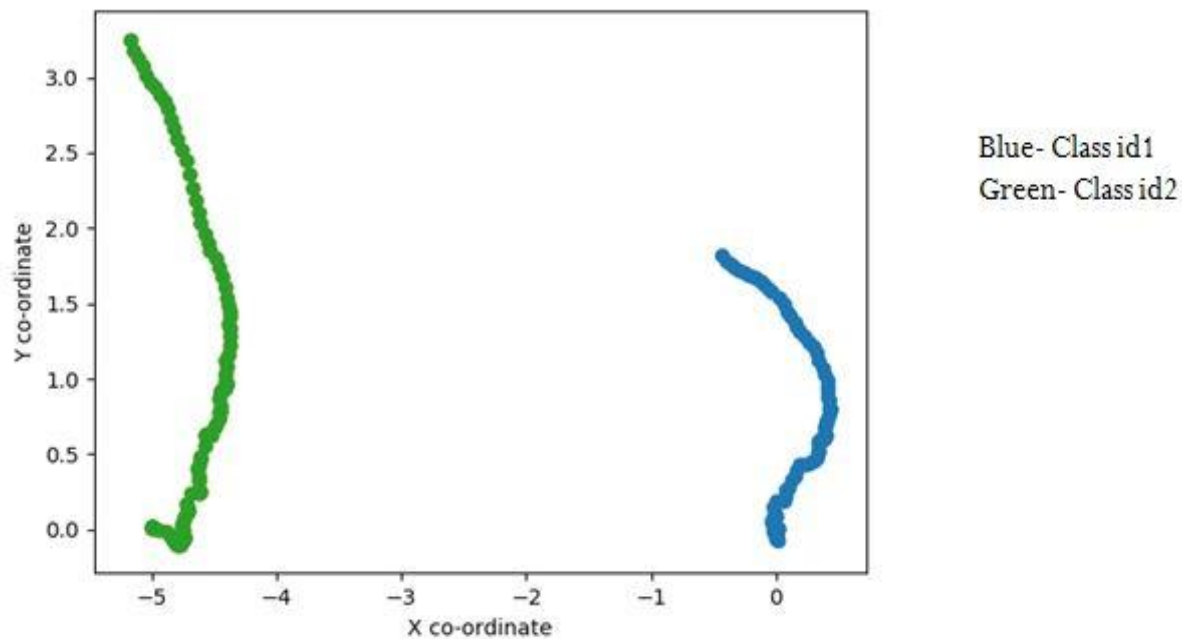


*Fig 13*: represents the trajectories followed by both the centrosomes (class id1 and 2) during the simulation period.

The trajectories of both the poles (represented as class id1 and id2) were traced in polar co-ordinates (Figure 5), which shows two different kinds of oscilations for two spindle oscillation. The spindle pole which doesn`t move much has some kind of damped oscilations, where the pole which moves vigorously has normal oscilations.
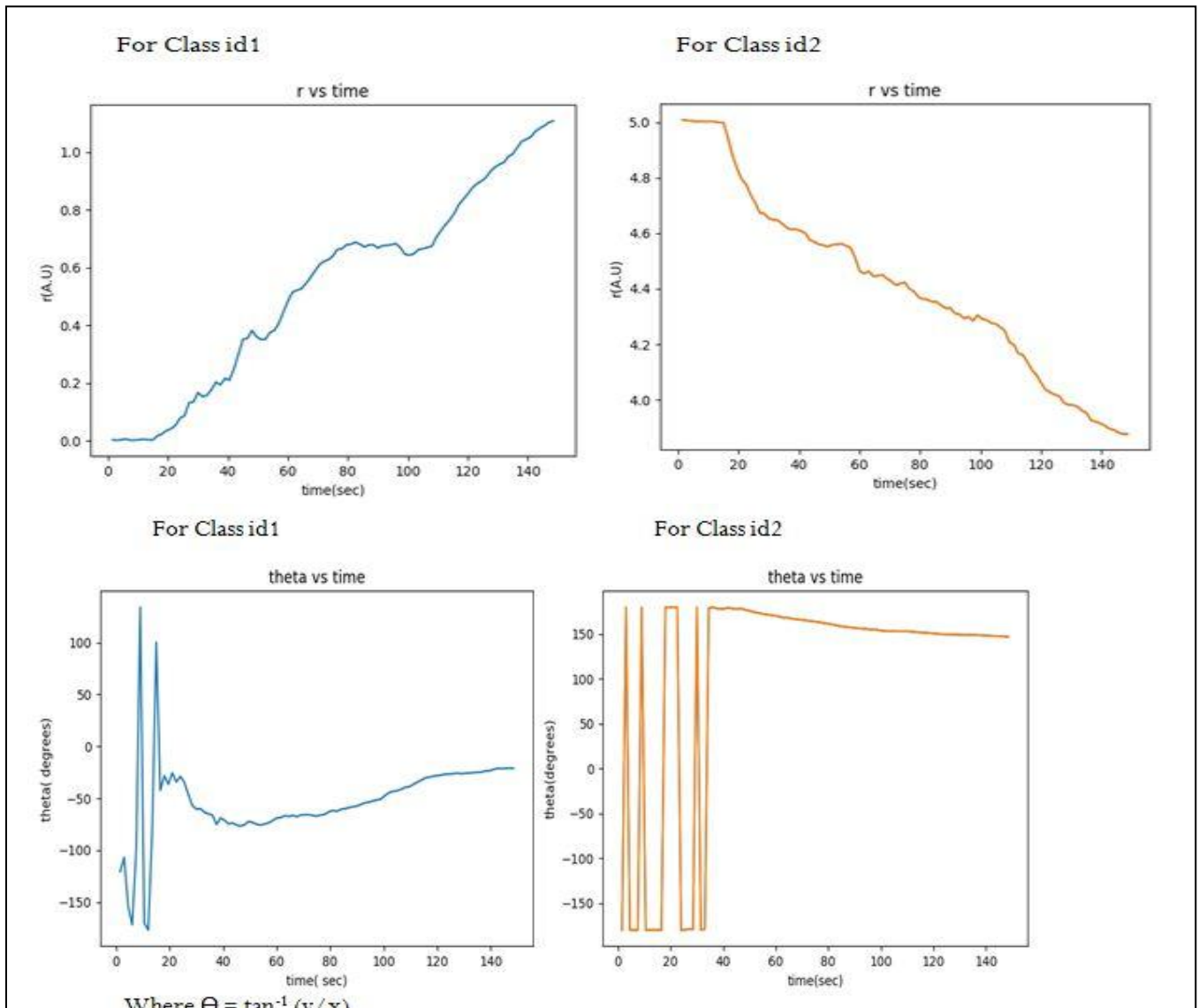


Where $\Theta = \tan^{-1} (y/x)$

Figure 14 represents the spindle movements in polar co-ordinates for class id 1 and class id 2 (centrosomes), where

$r = \text{sqrt} (x^2 + y^2)$ and $\Theta = \tan^{-1} (y/x)$.

**DISCUSSION:**

With the above explained methods and procedures we managed to get the viscosity values for the control samples, which were fairly comparable to the theoretical values. So, we proceeded with calculation of the viscosity values for the nematode species, which are unknown except for *C.elegans*. The viscosity value for *C.elegans* however doesn`t match with the reported value given by Daniel et al, 2003. However the hypothesis that we implemented about the difference in viscosity might lead to the different spindle motion and oscillation, still kind of holds true. Because, according to our hypothesis *Diploscapter* species should have significantly higher viscosity values as it shows the least movements of lipid granules in the time lapse series, which can be inferred from the bar graph shown in figure 9. *O. tipulae* has the lowest value for viscosity. The three different methods for MSD calculations, do give different values of viscosities for each species ($\eta$ of *Diploscapter* > *C. elegans* >*O. tipulae)*. The msdanalyzer method gives the highest value of viscosity for *Diploscaapter.*

The limitations to these methods are as follows: the manual tracking of the beads and lipid granules are tiring and time consuming. Moreover, in case of lipid granules, manual tracking becomes really difficult as the granules diffuse quickly and it gets difficult to track them for longer time frames. The MSD calculations and the fits to the mean MSD curves needs to more accurate. To improve the measurements we need more data sets (at least 50 granules) and for longer time frames. We need to calculate the MSD by using Perrin/Stoke-Einstein's method, for the optimization of the results in the estimation of viscosity.

So, now the question lies, if not viscosity, what other parameter or several parameters all together, lead to this evolutionary conserved phenomenon of asymmetric cell division and different spindle oscillations. The other parameters which can potentially affect this phenomenon have been described in table 3 given by Nedelec et al, 2007. So, with the improvisations of the Cytosim code, we can check for the effects of these parameters on the cell division and spindle oscillations in an *in vitro* scenario. The aspects of changes in the Cytosim code includes localization of motors on the cortex in an

asymmetric manner, quantification of the spindle oscillation, developing an optimized model for the different nematode species with respect to tuning different parameters.

References:

Bingham, Eugene Cook, and Richard Fay Jackson (1917). *Standard substances for the calibration of viscometers*. US Government Printing Office,

Cluet, D., Stébé, P. N., Riche, S., Spichty, M., & Delattre, M. (2014). Automated high-throughput quantification of mitotic spindle positioning from DIC movies of caenorhabditis embryos. *PloS one*, *9*(4), e93718.

Colombo, K., Grill, S. W., Kimple, R. J., Willard, F. S., Siderovski, D. P., & Gönczy, P. (2003). Translation of polarity cues into asymmetric spindle positioning in Caenorhabditis elegans embryos. *Science*, *300*(5627), 1957-1961.

Daniels, Brian R. et al. (2006) Probing Single-Cell Micromechanics In Vivo: The Microrheology of *C. elegans* Developing Embryos. Biophysical Journal , Volume 90 , Issue 12 , 4712 – 4719

Daniels, B. R., Masi, B. C., & Wirtz, D. (2006). Probing single-cell micromechanics in vivo: the microrheology of C. elegans developing embryos. *Biophysical journal*, *90*(12), 4712-4719.

Farhadifar, R., Baer, C. F., Valfort, A. C., Andersen, E. C., Müller-Reichert, T., Delattre, M., & Needleman, D. J. (2015). Scaling, selection, and evolutionary dynamics of the mitotic spindle. *Current biology*, *25*(6), 732-740.

Farhadifar, R., & Needleman, D. (2014). Automated segmentation of the first mitotic spindle in differential interference contrast microcopy images of C. elegans embryos. In *Mitosis* (pp. 41-45). Humana Press, New York, NY.

Glotzer, M. (2001). Animal cell cytokinesis. *Annual review of cell and developmental biology*, *17*(1), 351-386.

Gönczy, P., Schnabel, H., Kaletta, T., Amores, A. D., Hyman, T., & Schnabel, R. (1999). Dissection of cell division processes in the one cell stage Caenorhabditis elegans embryo by mutational analysis. *The Journal of cell biology*, *144*(5), 927-946.

Grill, S. W., Howard, J., Schäffer, E., Stelzer, E. H., & Hyman, A. A. (2003). The distribution of active force generators controls mitotic spindle position. *Science*, *301*(5632), 518-521.

I. F. Sbalzarini and P. Koumoutsakos. Feature Point Tracking and Trajectory Analysis for Video Imaging in Cell Biology, Journal of Structural Biology 151(2):182-195, 2005.

Karin Kiontke, David H.A Fitch- The phylogenetic relationships of Caenorhabditis and other rhabditis (August 11, 2005), Wormbook, ed. The *C. elegans* Research Community, Wormbook, doi/10.1895/wormbook.1.11.1.

Khetan, N., & Athale, C. A. (2016). A Motor-Gradient and Clustering Model of the Centripetal Motility of MTOCs in Meiosis I of Mouse Oocytes. *PLoS computational biology*, *12*(10), e1005102.

Kozlowski, C., Srayko, M., & Nedelec, F. (2007). Cortical microtubule contacts position the spindle in C. elegans embryos. *Cell*, *129*(3), 499-510.

Lesilee Rose and Pierre Gonczy, Polarity establishment, asymmetric division and segregation of fate determinants in early *C. elegans* embryos (December 30,2014), Wormbook, ed. The  *C. elegans* Research Community, Wormbook, doi/10.1895/wormbook.1.30.2.

Munro, E., Nance, J., & Priess, J. R. (2004). Cortical flows powered by asymmetrical contraction transport PAR proteins to establish and maintain anterior-posterior polarity

in the early C. elegans embryo. *Developmental cell*, *7*(3), 413-424.

Park, D. H., & Rose, L. S. (2008). Dynamic localization of LIN-5 and GPR-1/2 to cortical force generation domains during spindle positioning. *Developmental biology*, *315*(1), 42-54.
Pecreaux, J., Röper, J. C., Kruse, K., Jülicher, F., Hyman, A. A., Grill, S. W., & Howard, J. (2006). Spindle oscillations during asymmetric cell division require a threshold number of active cortical force generators. *Current Biology*, *16*(21), 2111-2122.

Segur, J. B., & Oberstar, H. E. (1951). Viscosity of glycerol and its aqueous solutions. *Industrial & Engineering Chemistry*, *43*(9), 2117-2120.

Srayko, Martin et al.(2005) Identification and Characterization of Factors Required for Microtubule Growth and Nucleation in the Early *C. elegans* Embryo. Developmental Cell , Volume 9 , Issue 2 , 223 – 236

Tarantino, N., Tinevez, J. Y., Crowell, E. F., Boisson, B., Henriques, R., Mhlanga, M., & Laplantine, E. (2014). TNF and IL-1 exhibit distinct ubiquitin requirements for inducing NEMO–IKK supramolecular structures. *J Cell Biol*, *204*(2), 231-245.

Valfort, A. C., Launay, C., Sémon, M., & Delattre, M. (2018). Evolution of mitotic spindle behavior during the first asymmetric embryonic division of nematodes. *PLoS biology*, *16*(1), e2005099.